

$SU(2)_{\text{CMB}}$ at high redshifts and the value of H_0

Steffen Hahn¹ and Ralf Hofmann²

¹ *Karlsruhe Institute of Technology
Hermann-von-Helmholtz-Platz 1
D-76344 Eggenstein-Leopoldshafen
Germany*

² *Institut für Theoretische Physik
Universität Heidelberg
Philosophenweg 16
69120 Heidelberg, Germany*

Abstract

We investigate a high- z cosmological model to compute the co-moving sound horizon r_s at baryon freeze-out following hydrogen recombination. This model assumes a replacement of the conventional CMB photon gas by $SU(2)$ Yang-Mills thermodynamics, three flavors of massless neutrinos ($N_\nu = 3$), and a *purely baryonic* matter sector (no cold dark-matter (CDM)). Relying on a realistic simulation of the ionization history throughout recombination, we obtain $z_* = 1720.98 \pm 6.45$ and $z_{\text{drag}} = 1847.96 \pm 7.46$. We give arguments why we believe that it is z_* rather than z_{drag} that determines baryon freeze-out in the new model. With $r_s(z_*) = (135.44 \pm 0.56)$ Mpc and the essentially model independent extraction of $r_s \times H_0 = \text{const}$ from low- z data in arXiv:1607.05617 we obtain a good match with the value $H_0 = (73.24 \pm 1.74) \text{ km s}^{-1} \text{ Mpc}^{-1}$ extracted in arXiv:1604.01424 by appealing to Cepheid calibrated SNe Ia, new parallax measurements, stronger constraints on the Hubble flow, and a refined computation of distance to NGC4258 from maser data. We briefly comment on a possible extension of our high- z model to match successful Λ CDM phenomenology at low z .

1 Introduction

The last two and a half decades have witnessed a tremendous industry in collecting and interpreting precise observational data to determine the cosmology of our Universe: (i) large-scale structure surveys confirming the existence of a standard ruler r_s set by the physics of baryonic acoustic oscillations (BAO) throughout the epochs preceding and including the recombination of primordial helium and hydrogen, e.g. [1, 2], (ii) observations of the cosmic microwave background (CMB), confirming its black-body nature and informing about CMB decoupling physics as well as associated primordial statistical properties of matter and hence temperature fluctuations, e.g. [3, 4, 5], and (iii) use of calibrated standard candles in luminosity distance-redshift observations, ultimately changing the paradigm on late-time expansion history (low- z regime) [6, 7]. As a consequence, we now appear to possess an accurate parametrisation of the Universe's composition in terms of the standard Λ CDM concordance model. Yet, we suspect that this model is prone to oversimplification: so far there is no falsifiable theory on what the dark sector actually is made of. Moreover, as we shall argue in the present work, the extrapolation of the observationally well established low- z model to thermal expansion history well before CMB decoupling, although seemingly in accord with the results of [4, 5], can be misleading.

In [8] the implication of a new SU(2) Yang-Mills theory describing the CMB towards its temperature-redshift (T - z) relation was analysed within an FLRW Universe. Due to non-conformal scaling at low z this relation suffers a lower linear slope at high z ($z \gtrsim 9$) compared to the standard U(1) theory,

$$\frac{T}{T_0} = z + 1, \quad (\text{U}(1), \forall z) \longrightarrow \quad \frac{T}{T_0} = 0.62(z + 1), \quad (\text{SU}(2)_{\text{CMB}}, z \gtrsim 9), \quad (1)$$

see also Fig. 1. We refrain here from reviewing the thermodynamics of an SU(2) Yang-Mills theory in its deconfining phase. We also skip a discussion of why the critical temperature $T_c = T_0$ ($T_0 = 2.725$ K referring to the present CMB temperature) for the onset of the deconfining-preconfining phase transition in such a theory is fixed by low-frequency observation of the present CMB, justifying the name $\text{SU}(2)_{\text{CMB}}$. To be informed about all this in a pragmatically fast way we refer the reader to [8], for an in-depth read we propose Ref. [9]. We do mention though that the standard relation between neutrino temperature T_ν and T , $T_\nu = (4/11)^{1/3}$, obtained from entropy conservation during e^+e^- annihilation, modifies in $\text{SU}(2)_{\text{CMB}}$ to

$$\frac{T_\nu}{T} = \left(\frac{g_1}{g_0} \right)^{1/3} = \left(\frac{16}{23} \right)^{1/3}. \quad (2)$$

This is because $g_0 = 8 + (7/8)4$ (number of relativistic degrees of freedom (d.o.f.) before annihilation) and $g_1 = 8$ (number of relativistic d.o.f. after annihilation), see [8]. Note that for, say, $z > 100$ $\text{SU}(2)_{\text{CMB}}$'s two massive vector excitations V^\pm can

be considered highly relativistic. Namely, at $z = 100$ one has $m_{V^\pm}/T \sim 1.4 \times 10^{-3}$ such that the energy density $\rho_{\text{SU}(2)_{\text{CMB}}}$ is due to eight relativistic d.o.f.

Because of relation (1) CMB decoupling sets in at a redshift of ~ 1800 which is highly disparate from $z \sim 1100$ purported by the Λ CDM concordance model. As discussed in [8], this suggests that at CMB decoupling the role of non-relativistic matter in Λ CDM cosmology, composed of cold dark and baryonic portions, is played solely by the baryons. The emergence of the dominant components in the established low- z cosmic mix, which are associated with a cold-dark-matter equation of state $p_{\text{CDM}} = 0$ and a dark-energy equation of state $p_\Lambda = -\rho_\Lambda$, through damped oscillations of, e.g., a Planck-scale axion field [10, 11] is an intriguing possibility. This is because such a field relates present vacuum energy (axion potential) to a quantum (chiral) anomaly [12, 13, 14, 15] at the Planck scale, invoked by topologically nontrivial gauge-field configurations (caloron and anticalorons [16, 17, 18, 19]) composing the thermal ground state of $\text{SU}(2)_{\text{CMB}}$. In particular, the axion potential is radiatively protected. To clarify whether such a scenario can explain the observed rotation curves of spiral galaxies and the extensive data on structure formation in terms of topologically stabilized, axially symmetric defects of the axion field [20] – seeded by Planckian physics and/or phase transitions in the early Universe – much more work is required.

The present paper therefore adopts the point of view that for cosmological purposes the Λ CDM model is a useful and accurate approximation to the actual physics for $z \lesssim 9$. At the same time, we suspect that for higher values of z this model increasingly fails because of relation (1). Fortunately, our high- z cosmological model, which is conservative concerning its (solely baryonic) matter content and the number of massless neutrino flavours but invokes $\text{SU}(2)_{\text{CMB}}$ to describe the CMB itself, can be tested in terms of the most basic low- z cosmological parameter: today's value of the cosmic expansion rate H_0 . This test of the high- z model heavily relies on an inverse proportionality between the co-moving sound horizon at baryon freeze-out r_s and H_0 , which was extracted from low- z data (Cepheid calibrated SNe Ia, new parallax measurements, stronger constraints on the Hubble flow, and a refined computation of distance to NGC4258 from maser data) under no model assumptions other than spatial flatness, SNe Ia/ r_s yielding standard candles/a standard ruler, and a smooth expansion history [21]. Obviously, this knowledge is important because it allows a high- z extraction of r_s to rule value H_0 . Note that the value of H_0 , as obtained by CMB analysis based on Λ CDM and U(1) photons [22], is at 3.4σ tension with the direct measurement of H_0 in [23].

When (re-)computing r_s in the new, high- z $\text{SU}(2)_{\text{CMB}}$ based model with $N_\nu = 3$ massless neutrinos, $T_0 = 2.725$ K, and solely baryonic matter (referred to $\text{SU}(2)_{\text{CMB}}$ in the following) and in the Λ CDM model we consider the parameter values of η_{10} , Y_P , N_{eff} , and Ω_{CDM} of [22] as representative, see Sec. 2.

This work is organized as follows. In Sec. 2 we introduce our high- z cosmological model and discuss the parameter setting, relying on the 2015 Planck results. A rough estimate of the decoupling redshift z_{dec} , obtained by assuming (i) thermalization

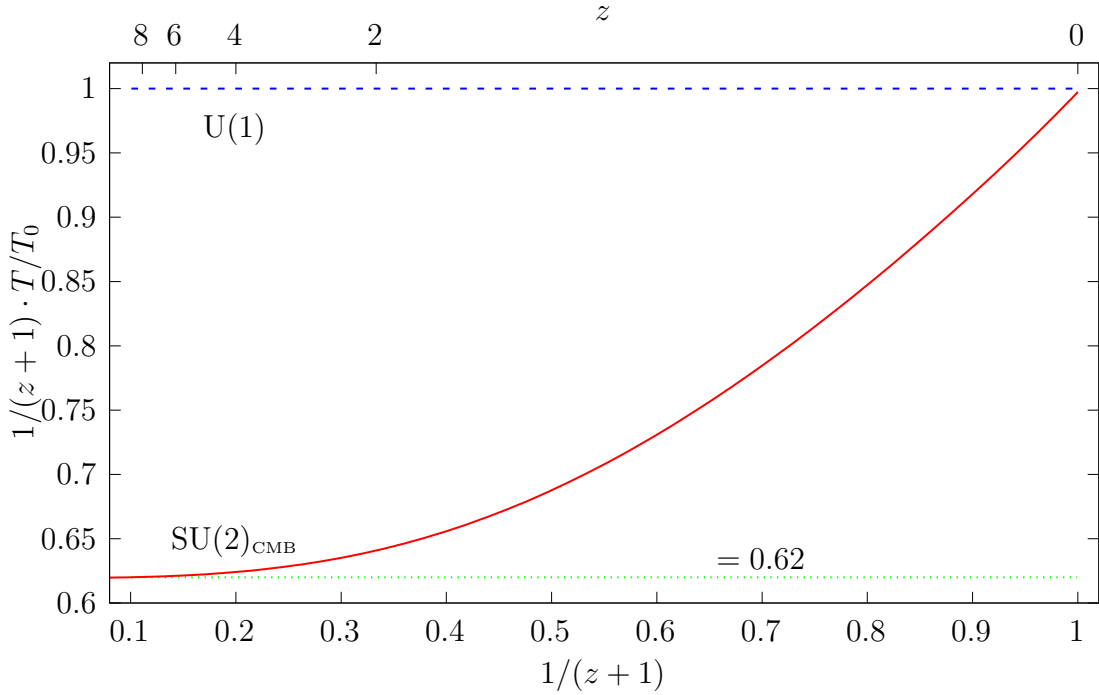


Figure 1: The $T - z$ scaling relation $T/(T_0(z+1))$ in $SU(2)_{\text{CMB}}$ (solid, red). Note the emergence of $T/T_0 = 0.62(z+1)$ for $z \gtrsim 9$ (dotted, green). The conventional $U(1)$ theory for thermal photon gases associates with the dashed, blue line. Data taken from [8].

(Saha equation) and (ii) instantaneous decoupling, is carried out for both $SU(2)_{\text{CMB}}$ and ΛCDM in Sec. 3. Comparing our value for z_{dec} with the realistic values for z_* and z_{drag} in ΛCDM , we conclude that this approximation systematically over-estimates the true redshifts for decoupling and baryon freeze-out. This led us to perform a realistic simulation of the recombination physics in Sec. 4 based on the Boltzmann code `recfast`, the simulation for ΛCDM serving as a check in reproducing the values for $r_s(z_{\text{drag}})$ and $r_s(z_*)$ of [22]. We find that for $SU(2)_{\text{CMB}}$ $z_{\text{drag}} > z_*$. We give arguments why, in contrast to ΛCDM , it is z_* which sets the redshift for baryon freeze-out in $SU(2)_{\text{CMB}}$. Subsequently, we compute $r_s(z_*)$ and $r_s(z_{\text{drag}})$. With the $r_s - H_0$ relation of [21] we deduce from our value of $r_s(z_*)$ a match of H_0 with the value given in [23]. In Sec. 5 we summarize our work and sketch a road map for future work. The Appendix contains a table documenting the changes in the `recfast` code when adapted to $SU(2)_{\text{CMB}}$.

2 High- z cosmological model and sound horizon

Let us introduce our high- z cosmological model $SU(2)_{\text{CMB}}$. As usual, a subscript "0" refers to today's value of the associated quantity, we work in super-natural units,

where $c = \hbar = k_B = 1$, and we assume a spatially flat FLRW Universe such

$$H(z) = H_0 \sqrt{\sum_i \Omega_i(z)}, \quad (3)$$

with $\Omega_i(z = 0) \equiv \Omega_{i,0}$ defining the ratio of today's energy density $\rho_{i,0}$, inherent to the i th separately conserved (and at $z \gg 1$ relevant) cosmic fluid, to today's critical density $\rho_{c,0} \equiv 3/(8\pi G) H_0^2$. Here G denotes Newton's constant. Furthermore, we make the convention

$$H_0 \equiv h 100 \text{ km s}^{-1} \text{ Mpc}^{-1}. \quad (4)$$

We consider $N_\nu = 3$ flavours of massless neutrinos [24] to form a separately conserved cosmic fluid. Because of $\text{SU}(2)_{\text{CMB}}$ the neutrino temperature T_ν is determined by the CMB temperature T as in Eq. (2), and their energy density ρ_ν relates to the energy density of CMB photons ρ_γ as

$$\rho_\nu(T) = \frac{7}{8} \left(\frac{16}{23} \right)^{4/3} N_\nu \rho_\gamma(T). \quad (5)$$

Because eight instead of two relativistic d.o.f. determine the energy density $\rho_{\text{SU}(2)_{\text{CMB}}}$ (in distinction to ρ_γ !) at high- z one has

$$\rho_{\text{SU}(2)_{\text{CMB}}}(T) = 4 \rho_\gamma(T). \quad (6)$$

Writing $\rho_{\text{SU}(2)_{\text{CMB}}}$ as a function of z , Eq. (1) implies

$$\rho_{\text{SU}(2)_{\text{CMB}}}(z) = A \rho_{\gamma,0}(z+1)^4, \quad (7)$$

where

$$A \equiv (8/2) \cdot (0.62)^4 = 0.59105. \quad (8)$$

Considering Eq. (3), Eqs. (7) and (5) are recast as

$$\rho_{\text{SU}(2)_{\text{CMB}}}(z) = A H_0^2 \Omega_{\gamma,0}(z+1)^4, \quad (9)$$

and

$$\rho_\nu(z) = \frac{7}{8} \frac{A}{4} \left(\frac{16}{23} \right)^{4/3} N_\nu H_0^2 \Omega_{\gamma,0}(z+1)^4. \quad (10)$$

Setting $T_0 = 2.725 \text{ K}$ [25], one has $\Omega_{\gamma,0} = 2.46796 \times 10^{-5} h^{-2}$.

Non-relativistic, cosmological matter is assumed to be purely baryonic in $\text{SU}(2)_{\text{CMB}}$. Its energy density today, $\rho_{b,0}$, relates to $\rho_{\gamma,0}$ as

$$\rho_{b,0} = \frac{4}{3} R_0 \rho_{\gamma,0} \quad (11)$$

such that

$$R_0 \equiv 111.019 \eta_{10}. \quad (12)$$

From Big-Bang Nucleosynthesis (BBN) η_{10} is constrained to $4.931 \leq \eta_{10} \leq 7.123$, see Fig. 29 in [26]. The number η_{10} parametrizes today's baryon-to-photon number-density ratio $n_{b,0}/n_{\gamma,0}$ as

$$n_{b,0}/n_{\gamma,0} \equiv \eta_{10} \times 10^{-10}. \quad (13)$$

Note that the central value in

$$\eta_{10} = 6.08232 \pm 0.06296, \quad (14)$$

as computed from the value $\Omega_b = (0.02222 \pm 0.00023) h^{-2}$, which is obtained by the Planck collaboration [22], is also central to the above BBN range. According to [22] this value of η_{10} implies a ${}^4\text{He}$ mass fraction Y_P of

$$Y_P = 0.252 \pm 0.041. \quad (15)$$

Note that due to non-conformal T - z scaling in $\text{SU}(2)_{\text{CMB}}$ there is a low- z dependence of n_b/n_{γ} – in contrast to the conventional case of $\text{U}(1)$ photons. Also, because of Eq. (1) the high- z expression for quantity R reads

$$R(z) \equiv 111.019 \frac{\eta_{10}}{(0.62)^4(z+1)}. \quad (16)$$

Taking the central value for η_{10} from Eq. (14), appealing to $T_{\text{dec}} \sim 3000$ K, and considering Eq. (1), we estimate the redshift z_{dec} for then end of hydrogen recombination as $z_{\text{dec}} \sim 3000/(0.62 \cdot 2.725) - 1 \sim 1775$. Therefore, we conclude from Eq. (12) that in $\text{SU}(2)_{\text{CMB}}$ $R(z) > 1$ for z ranging from $z = 0$ to well beyond recombination: $R(z) > 1$ for $z < 4568$. This is in contrast to the conventional ΛCDM model where CMB decoupling occurs at $z_{\text{dec}} \sim 1100$ and where R is given as

$$R(z) \equiv 111.019 \frac{\eta_{10}}{z+1} \quad (17)$$

such that $R(z) < 1$ for $z > 675$. It is suggestive that such a disparity in the behaviour of $R(z)$ between $\text{SU}(2)_{\text{CMB}}$ and ΛCDM has profound consequences for baryon freeze-out. We will come back to this issue in Sec. 4.

As usual we have

$$\frac{\rho_b(z)}{\rho_{c,0}} \equiv \Omega_{b,0}(z+1)^3, \quad (18)$$

where [22]

$$\Omega_{b,0} \equiv 0.00365321 \eta_{10} h^{-2}. \quad (19)$$

Therefore, in $\text{SU}(2)_{\text{CMB}}$ the high- z Hubble parameter H reads

$$H(z) = H_0 \left[\Omega_{b,0}(z+1)^3 + A \left(1 + \frac{7}{32} \left(\frac{16}{23} \right)^{4/3} N_{\nu} \right) \Omega_{\gamma,0}(z+1)^4 \right]^{1/2}, \quad (20)$$

Table 1: Cosmological high- z models: Λ CDM versus $SU(2)_{\text{CMB}}$.

	Λ CDM	$SU(2)_{\text{CMB}}$
$\frac{T}{T_0}$	$z + 1$	$0.62(z + 1)$
$\frac{T_\nu}{T}$	$\left(\frac{4}{11}\right)^{1/3}$	$\left(\frac{16}{23}\right)^{1/3}$
Ω_{CDM}	Ω_{CDM}	0
N_ν	N_{eff}	3

where $\Omega_{b,0}$ and its errors derive from η_{10} as quoted in Eq. (14). We also consider the high- z Λ CDM model

$$H(z) = H_0 \left[(\Omega_{b,0} + \Omega_{\text{CDM}}) (z + 1)^3 + \left(1 + \frac{7}{8} \left(\frac{4}{11} \right)^{4/3} N_{\text{eff}} \right) \Omega_{\gamma,0} (z + 1)^4 \right]^{1/2}, \quad (21)$$

where according to [22] we have

$$\Omega_{\text{CDM}} = (0.1197 \pm 0.0022) h^{-2}, \quad N_{\text{eff}} = 3.15 \pm 0.23. \quad (22)$$

Note that in both cases, Eqs. (20) and (21), the high- z expressions for $H(z)$ are independent of h . An overview of the differences between high- z Λ CDM and $SU(2)_{\text{CMB}}$ is presented in Tab. 1.

The sound horizon $r_s(z)$, as emergent within the baryon-photon plasma, is defined as

$$r_s(z) = \int_0^{\eta(z)} d\eta' c_s(\eta') = \int_z^\infty dz' \frac{c_s(z')}{H(z')}, \quad (23)$$

where η is conformal time ($d\eta \equiv dt/a$), and c_s denotes the sound velocity, given as

$$c_s \equiv \frac{1}{\sqrt{3(1 + R)}}. \quad (24)$$

In Eq. (24) R either needs to be taken from Eq. (12) ($SU(2)_{\text{CMB}}$) or from Eq. (17) (Λ CDM).

Finally, we would like to explain how we perform error estimates for $r_s(z)$. For example, in $SU(2)_{\text{CMB}}$ error-prone input parameters are η_{10} and Y_P . For those we generate pairs of Gaussian distributed random values. For each pair we compute $r_s(z)$ and fit a Gaussian to the ensuing histogram in order to extract the $1-\sigma$ error range for $r_s(z)$. In doing this, z needs to satisfy a condition, specified either by Eqs. (34), (37), or (39), to determine its value z_{dec} , z_* , and z_{drag} , respectively. For Λ CDM the set $\{\eta_{10}, Y_P\}$ is enhanced by the elements Ω_{CDM} and N_{eff} . For an overview of the values of the cosmological parameters see Tab. 2.

Table 2: Cosmological parameter values employed in the computations and their sources.

parameter	value	source
H_0 ($SU(2)_{\text{CMB}}$)	$(73.24 \pm 1.74) \text{ km s}^{-1} \text{ Mpc}^{-1}$	[23]
H_0 (ΛCDM)	$(67.31 \pm 0.96) \text{ km s}^{-1} \text{ Mpc}^{-1}$	TT+lowP, [22]
T_0	2.725 K	[25]
$\Omega_{\gamma,0}h^2$	2.46796×10^{-5}	based on $T_0 = 2.725$ K
$\Omega_{b,0}h^2$	0.02222 ± 0.99923	TT+lowP, [22]
$\Omega_{\text{CDM},0}h^2$	0.1197 ± 0.0022	TT+lowP, [22]
η_{10}	6.08232 ± 0.06296	based on $\Omega_{\gamma,0}h^2$, TT+lowP, [22]
Y_P	0.252 ± 0.041	TT, [22]
N_{eff}	3.15 ± 0.23	abstract, [22]

3 Saha equation and instantaneous CMB decoupling/radiation drag

Before we turn to a detailed analysis of recombination physics in Sec. 4, let us now perform a rough estimate for a single redshift z_{dec} associated with CMB decoupling physics/radiation drag. In the present section, we base our estimate on two assumptions: (i) thermalization (Saha equation) and (ii) coincidence of decoupling and radiation drag, both of vanishing duration.

Appealing to the results of [21] on the low- z inverse proportionality between the sound horizon r_s , seen in today's baryonic matter correlation, and H_0 , our here-determined central value of H_0 for ΛCDM over-estimates the result

$$H_0 = (67.31 \pm 0.96) \text{ km s}^{-1} \text{ Mpc}^{-1} \quad (25)$$

of [22]. Also, our estimate of H_0 for $SU(2)_{\text{CMB}}$ is higher than the directly measured value

$$H_0 = (73.24 \pm 1.74) \text{ km s}^{-1} \text{ Mpc}^{-1} \quad (26)$$

of [23]. This motivates our analysis of Sec. 4.

In the present section, the value of z_{dec} is determined from condition

$$H(z_{\text{dec}}) = \Gamma(z_{\text{dec}}). \quad (27)$$

In Eq. (27) the rate Γ for scattering of eV-photons off free, non-relativistic electrons reads

$$\Gamma = \sigma_T n_e^b \chi_e, \quad (28)$$

where $\sigma_T \equiv 6.65 \times 10^{-25} \text{ cm}^2$ denotes the Thomson cross section for electron-photon scattering, n_e^b is the electron density just before the onset of hydrogen recombination

which is given as

$$n_e^b(z) \equiv (1 - Y_P) n_b(z) = 410.48 \cdot 10^{-10} \eta_{10} (1 - Y_P) (z + 1)^3 \text{ cm}^{-3}. \quad (29)$$

Moreover, χ_e refers to the ionization fraction during the recombination epoch,

$$\chi_e(z) \equiv \frac{n_e(z)}{n_e^b(z)}, \quad (30)$$

n_e being the actual electron density, evolving in principle non-trivially during recombination, see Sec. 4. In our present treatment we set $z = z_{\text{dec}}$ in Eqs. 29 and 30. We also use the Saha equation, which appeals to thermal equilibrium between electrons, photons, and ions¹

$$\frac{\chi_e^2}{1 - \chi_e} = \frac{1}{n_e^b} \left(\frac{T_{\text{dec}} m_e}{2\pi} \right)^{3/2} \exp \left(-\frac{B_H}{T_{\text{dec}}} \right) \equiv S, \quad (31)$$

to estimate χ_e^2 at z_{dec} . In Eq. (31) the following values are set for the quantities m_e, B_H :

$$m_e = 510998.94 \text{ eV}, \quad B_H = 13.6 \text{ eV}. \quad (32)$$

Depending on whether the cosmological model of Eq. (20) ($\text{SU}(2)_{\text{CMB}}$) or Eq. (21) (ΛCDM) is considered, we set in Eq. (31) $T_{\text{dec}} = 0.62(z_{\text{dec}} + 1)T_0$ or $T_{\text{dec}} = (z_{\text{dec}} + 1)T_0$, respectively. Solving Eq. (31) for χ_e , we have

$$\chi_e = \frac{1}{2} [-S + S^{1/2}(4 + S)^{1/2}] \sim S^{1/2} \quad (S \ll 1). \quad (33)$$

On the other hand, solving Eq. (27) for χ_e yields

$$\chi_e(z_{\text{dec}}) = \frac{1}{\sigma_T n_e^b(z_{\text{dec}})} H(z_{\text{dec}}), \quad (34)$$

where either the expression in Eq. (20) ($\text{SU}(2)_{\text{CMB}}$) or Eq. (21) (ΛCDM) is substituted for H . Equating the right-hand sides of Eq. (33) and Eq. (34) as foreseen by Eq. (27), we derive approximate values for z_{dec} and their errors from $\eta_{10}, Y_P, \Omega_{\text{CDM}}$, and N_{eff} as quoted in Eqs. (14), (15), and (22), respectively, see also Tab. 2. We obtain

$$\begin{aligned} z_{\text{dec}} &= 1787.58 \pm 1.86 & (\text{SU}(2)_{\text{CMB}}), \\ z_{\text{dec}} &= 1132.78 \pm 1.27 & (\Lambda\text{CDM}). \end{aligned} \quad (35)$$

Appealing to Eq. (23), we arrive at

$$\begin{aligned} r_s(z_{\text{dec}}) &= (131.97 \pm 0.45) \text{ Mpc} & (\text{SU}(2)_{\text{CMB}}), \\ r_s(z_{\text{dec}}) &= (140.18 \pm 1.30) \text{ Mpc} & (\Lambda\text{CDM}), \end{aligned} \quad (36)$$

¹Thomson scattering off neutral hydrogen and Helium atoms can safely be neglected [27].

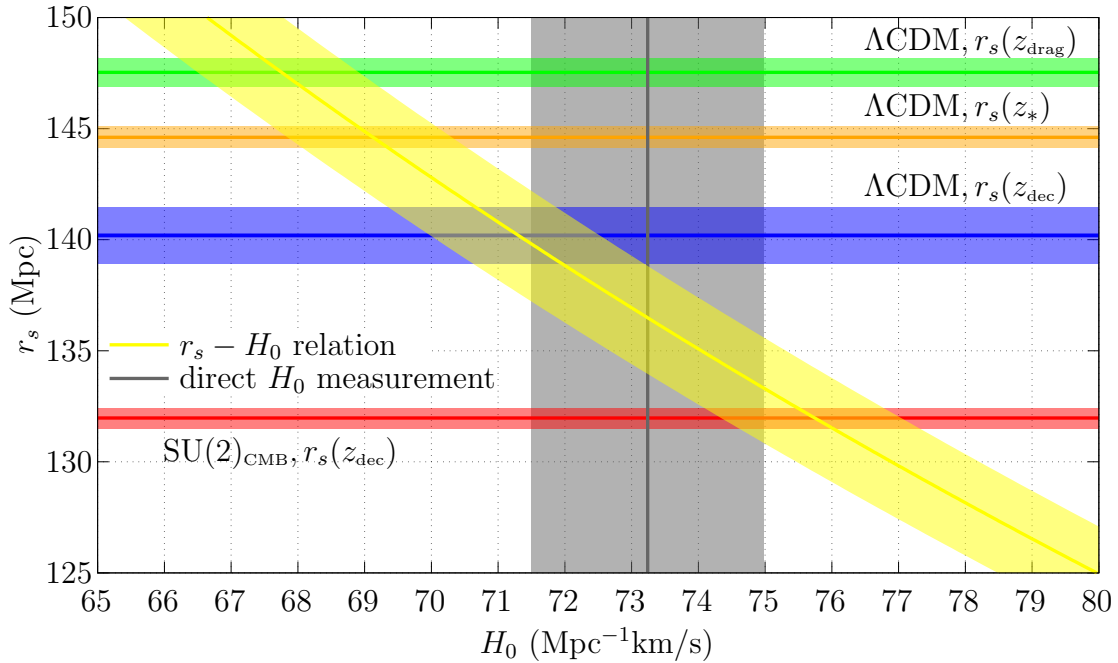


Figure 2: Instantaneous-decoupling predictions of the sound horizon r_s including the $1-\sigma$ error range in high- z Λ CDM (blue) and $SU(2)_{\text{CMB}}$ (red) together with the low- z r_s - H_0 relation of [21] (yellow) and the direct measurement of H_0 as reported in [23] (grey). For completeness we also quote $r_s(z_{\text{drag}})$ and $r_s(z_*)$ in Λ CDM (green) and (orange), for definitions see Sec. 4.

see Fig. 2. Amusingly, the intersections of the bands $r_s(z_{\text{dec}})$ in $SU(2)_{\text{CMB}}$ and Λ CDM with the $r_s - H_0$ band of [21] have a non-vanishing intersection with the $1-\sigma$ range of H_0 measured in [23]. However, we observe that $r_s(z_{\text{dec}})$ is considerably under-estimated compared to $r_s(z_{\text{drag}})$ in Λ CDM. Therefore, we suspect that $r_s(z_{\text{dec}})$ is also under-estimated in $SU(2)_{\text{CMB}}$ compared to its true value at baryon freeze-out. Indeed, since $\chi_e(z_{\text{dec}}) = 0.003$ ($SU(2)_{\text{CMB}}$) and $\chi_e(z_{\text{dec}}) = 0.010$ (Λ CDM) we are left with considerable doubt on whether our present treatment yields reliable results.

4 Realistic treatment of recombination

Here we would like to subject recombination physics to realistic histories of the ionization fraction $\chi_e(z)$. We appeal to the publically available Boltzmann code `recfast` [28] which was also used in [26]. When computing $\chi_e(z)$ in $SU(2)_{\text{CMB}}$ the following code adjustments need to be performed: re-set fnu from $\text{fnu}=21/8 \times (4/11)^{4/3}$ to $\text{fnu}=21/8 \times (23/16)^{4/3}$ ($N_{\text{eff}} = 3 = N_\nu$ by default) and re-define ranges in z for treatments by Saha, Peebles, or Boltzmann equation through divisions by 0.62. Note that for a fixed value of Ω_b (and $\Omega_{\text{CDM}} = 0$) the value H_0 can be varied

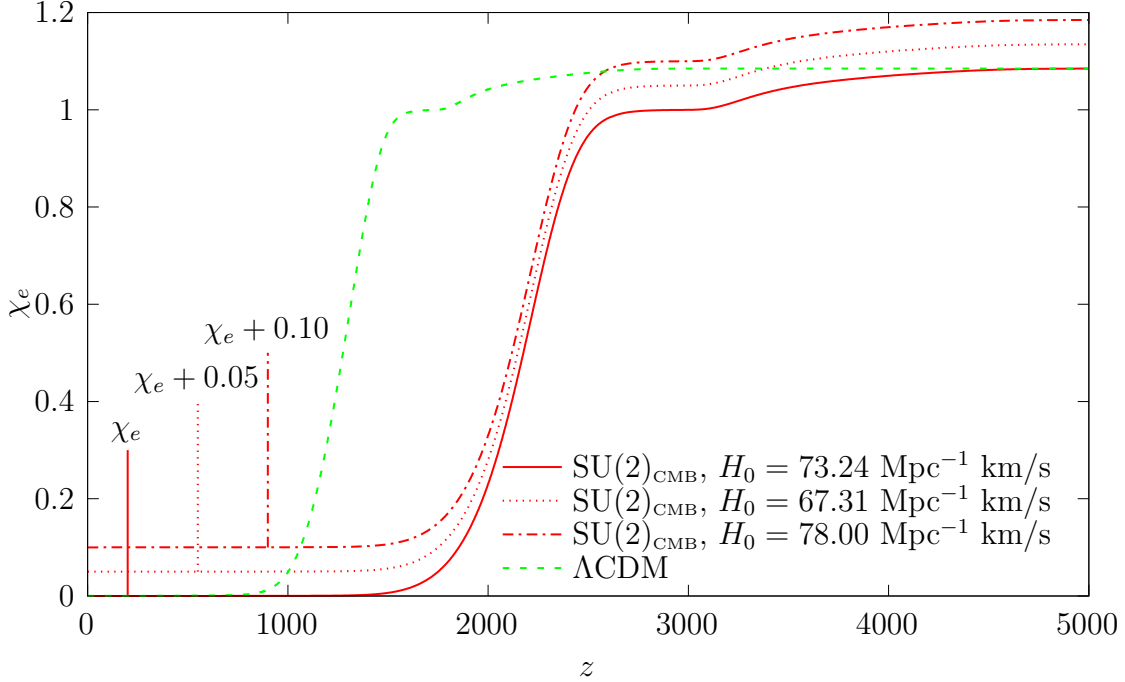


Figure 3: Histories for the ionization fraction $\chi_e(z)$ in $SU(2)_{\text{CMB}}$ (red with artificially introduced vertical offsets to distinguish curves for different values of H_0) and ΛCDM (green) subject to the parameter values defined in Tab. 2, see also Sec. 2. Regions, for which $\chi_e(z) > 1$, associate with incomplete Helium recombination.

in association with value of Ω_{vac} such that the curvature term in $H(z)$ is nil. For a exposition of important changes when going from ΛCDM to $SU(2)_{\text{CMB}}$, see Tab. 3 in the Appendix. Our results for $\chi_e(z)$ do not depend on H_0 , see Fig. 3. To define the end of recombination at z_* we apply the usual criterion of the optical depth $\tau(z_*)$ to Thomson scattering from $z = 0$ to z_* being equal to unity [26]. That is,

$$\tau(z_*) = \sigma_T \int_0^{z_*} dz \frac{\chi_e(z) n_e^b(z)}{(z+1)H(z)} = 1, \quad (37)$$

where $n_e^b(z)$ and $\chi_e(z)$ are defined in Eq. (29) and Eq. (30), respectively, and $H(z)$ either is given by Eq. (20) ($SU(2)_{\text{CMB}}$) or Eq. (21) (ΛCDM). To define the end of the radiation-drag epoch we follow [29] where it is argued that due to momentum conservation the asymptotic approach of baryon- and photon-fluid velocities occurs at a rate scaled by the factor R^{-1} of Eqs. (16) ($SU(2)_{\text{CMB}}$) and (17) (ΛCDM). This has prompted the definition of a radiation-drag depth $\tau_b(z)$ as

$$\tau_b(z) = \sigma_T \int_0^z dz' \frac{\chi_e(z') n_e^b(z')}{(z'+1)H(z')R(z')} . \quad (38)$$

The condition for freeze-out of the density fluctuations in baryonic matter at z_{drag} then is pronounced to be

$$\tau_b(z_{\text{drag}}) = 1. \quad (39)$$

Below we will question the physical relevance of condition (39) if $R > 1$ for z ranging from zero to well beyond recombination.

Using the parameter values of Sec. 2 and appealing to Eqs. (37) and (23), we obtain

$$\begin{aligned} z_* &= 1720.98 \pm 6.45 & (\text{SU(2)}_{\text{CMB}}), \\ z_* &= 1090.09 \pm 0.42 & (\Lambda\text{CDM}), \end{aligned} \quad (40)$$

and

$$\begin{aligned} r_s(z_*) &= (135.44 \pm 0.56) \text{ Mpc} & (\text{SU(2)}_{\text{CMB}}), \\ r_s(z_*) &= (144.61 \pm 0.49) \text{ Mpc} & (\Lambda\text{CDM}). \end{aligned} \quad (41)$$

On the other hand, Eqs. (38) and (23) yield

$$\begin{aligned} z_{\text{drag}} &= 1847.96 \pm 7.46 & (\text{SU(2)}_{\text{CMB}}), \\ z_{\text{drag}} &= 1059.57 \pm 0.46 & (\Lambda\text{CDM}), \end{aligned} \quad (42)$$

and

$$\begin{aligned} r_s(z_{\text{drag}}) &= (129.03 \pm 0.49) \text{ Mpc} & (\text{SU(2)}_{\text{CMB}}), \\ r_s(z_{\text{drag}}) &= (147.33 \pm 0.49) \text{ Mpc} & (\Lambda\text{CDM}). \end{aligned} \quad (43)$$

For $\text{SU(2)}_{\text{CMB}}$ we have

$$\chi_e(z_*) \sim 0.04, \quad \chi_e(z_{\text{drag}}) \sim 0.10. \quad (44)$$

From Eqs. (40) and (42) we learn that in $\text{SU(2)}_{\text{CMB}}$ a situation $z_{\text{drag}} > z_*$ arises. This is because $R > 1$ from $z = 0$ to well beyond recombination, see Sec. 2. But is z_{drag} in such a situation physically acceptable for baryon freeze-out? At z_{drag} , where χ_e is about 10%, see Eq. (44) or Fig. 3, baryons and photons are yet substantially coupled. As a consequence, their density fluctuations still propagate which is a more important effect than the Compton drag on individual, non-relativistic particle velocities. This, however, contradicts the idea of baryon freeze-out at z_{drag} . Thus, it is natural to proceed until CMB decoupling at z_* , freezing the *propagation* of baryonic fluctuations, with the Compton-drag effect subsequently taking over to brake down particle motion in the co-moving frame nearly instantaneously. We remark that due to the absence of cold dark matter in $\text{SU(2)}_{\text{CMB}}$ there are no external gravitational potential wells to pin baryonic fluctuations by infall. For $\text{SU(2)}_{\text{CMB}}$ we thus propose the redshift z_b for baryon freeze-out to be given as

$$z_b = \min\{z_*, z_{\text{drag}}\}. \quad (45)$$

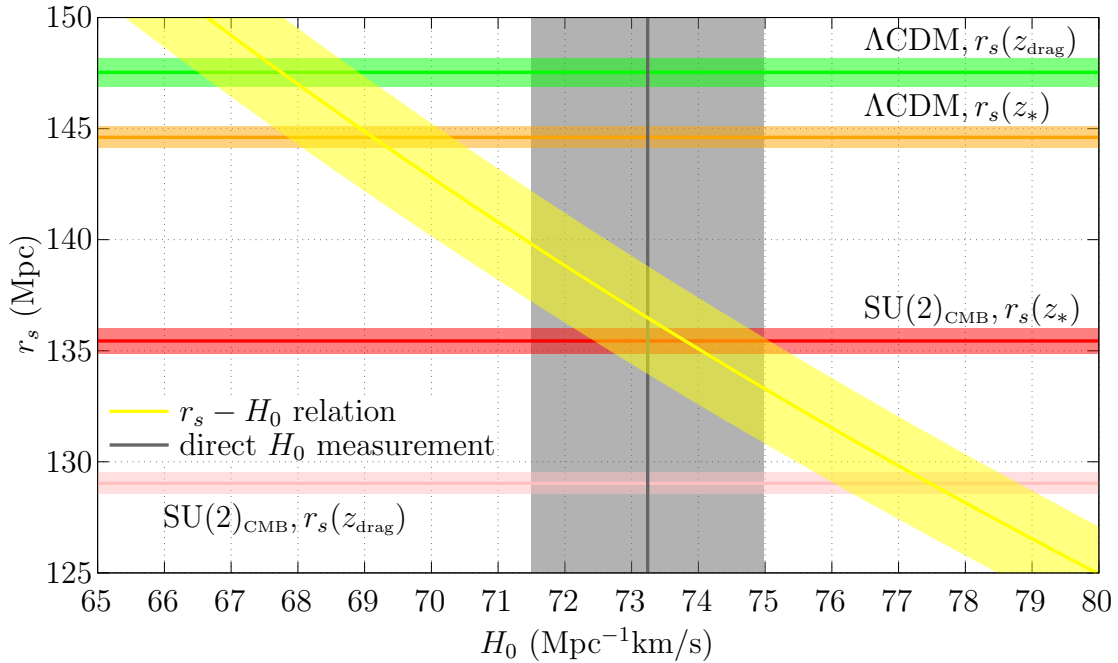


Figure 4: Predictions of the sound horizon r_s including the $1-\sigma$ error at z_* and z_{drag} in high- z ΛCDM (orange, green) and $\text{SU}(2)_{\text{CMB}}$ (red, pink) together with the low- z r_s - H_0 relation of [21] (yellow) and the direct measurement of H_0 as reported in [23] (grey).

The confrontation of Eqs. (41) and (43) with the low- z r_s - H_0 relation of [21] and the direct measurement of H_0 in [23] is depicted in Fig. 4.

While the intersection of the $\text{SU}(2)_{\text{CMB}}$ -band for $r_s(z_{\text{drag}})$ with the r_s - H_0 band of [21] is a bit off the $1-\sigma$ range of the directly measured value of H_0 [23] the intersection of the $\text{SU}(2)_{\text{CMB}}$ -band $r_s(z_*)$ is well contained within this $1-\sigma$ range.

5 Summary and Outlook

In the present work we have investigated whether a $3.4-\sigma$ discrepancy [21] in the value of the present Hubble parameter H_0 can be resolved under minimal assumptions concerning the high- z matter sector. This discrepancy relates to the value of H_0 as extracted by the Planck collaboration under an assumed all- z validity of the ΛCDM concordance model [22] and the value directly measured in [23]. As suggested by our results, a new, high- z cosmology, which assumes $\text{SU}(2)_{\text{CMB}}$ thermodynamics [9], solely baryonic matter, and $N_\nu = 3$ species of massless neutrinos, is a candidate. Our present analysis was enabled by a model-independent extraction of the r_s - H_0 relation (r_s the co-moving sound horizon in today's matter correlation function) which is based on low- z observation [21].

Interestingly, in the new model the redshift z_* , set by the end of hydrogen recombination, is preceded by the redshift z_{drag} governing the termination of the Compton drag effect. If, for reasons discussed in Sec. 4, we adopt the idea that hence it is z_* rather than z_{drag} to determine the freeze-out of baryonic matter fluctuations then we obtain good agreement with the directly measured value of H_0 [23], see Fig. 4.

As discussed in [21], the errors of such a direct measurement of H_0 will shrink substantially in the near future. Thus the here-proposed high- z cosmology will soon undergo increasingly stringent tests. Also, it remains to be investigated what the influence of this model on higher acoustic harmonics and the associated damping physics is. We believe that the incorporation of $\text{SU}(2)_{\text{CMB}}$ thermodynamics into the low- z cosmological model requires a match of the successful ΛCDM phenomenology to the “activation” of a nearly spatio-temporally homogeneous Planck-scale axion field φ (potential energy being the vacuum component in ΛCDM) [10, 11]. Such an activation concerns φ ’s coherent oscillations (CDM component in ΛCDM) and the properties of its solitonic defects (rotation curves of spiral galaxies) [20].

Once such a match can be performed a detailed addressation of the large-angle anomalies of the CMB is in order. Namely, as outlined in [30] and detailed in [9], radiative effects in $\text{SU}(2)_{\text{CMB}}$ (transverse and longitudinal contributions to the photon polarization tensor $\Pi_{\mu\nu}$), which are important at redshift $0.5 \leq z \leq 2$, induce a systematic departure from statistical isotropy. This is reflected by the build-up of a cosmologically local temperature depression (due to the transverse part of $\Pi_{\mu\nu}$), defining a gradient to its slope. The associated mild breaking of isotropy in the CMB temperature map would influence both the low lying CMB multipoles as well as the late-time emergence of intergalactic magnetic fields (due to the longitudinal part of $\Pi_{\mu\nu}$).

Acknowledgments

We would like to thank Jose Luis Bernal and Adam Riess for providing us with their data files on the low- z $r_s - H_0$ relation and the direct measurement of H_0 .

Appendix: Code adjustments in `recfast`

Table 3: Differences in `recfast` code of [31] for ΛCDM versus $\text{SU}(2)_{\text{CMB}}$. For a given code line (first column) the first (second) line in second column corresponds to ΛCDM ($\text{SU}(2)_{\text{CMB}}$).

line	recfast
356	<code>fnu = (21.d0/8.d0)*(4.d0/11.d0)**(4.d0/3.d0)</code>
	<code>fnu = (21.d0/8.d0)*(16.d0/23.d0)**(4.d0/3.d0)</code>

Continued on next page

Table 3 – continued from previous page

line	recfast
358	$z_eq = (3.0d0 * (H0*C)**2 / (8.0d0 * Pi * G * a * (1.0d0 + fnu) * Tnow**4)) * 0megaT$
	$z_eq = (3.0d0 * (H0*C)**2 / (8.0d0 * Pi * G * a * (4.0d0 + fnu) * (Tnow * 0.62d0)**4)) * 0megaT$
421	$y(3) = Tnow * (1.0d0 + z)$
	$y(3) = Tnow * (1.0d0 + z) * 0.62d0$
462	if (zend.gt.8000.d0) then
	if (zend.gt.13000.d0) then
469	$y(3) = Tnow * (1.0d0 + z)$
	$y(3) = Tnow * (1.0d0 + z) * 0.62d0$
471	else if(z.gt.5000.d0) then
	else if(z.gt.8000.d0) then
475	$rhs = dexp(1.5d0 * dLog(CR*Tnow/(1.0d0+z)))$
	$rhs = dexp(1.5d0 * dLog(CR*Tnow*0.62d0/(1.0d0+z)))$
476	$- CB1_He2 / (Tnow * (1.0d0+z)) / Nnow$
	$- CB1_He2 / (Tnow * (1.0d0+z) * 0.62d0) / Nnow$
482	$y(3) = Tnow * (1.0d0 + z)$
	$y(3) = Tnow * (1.0d0 + z) * 0.62d0$
484	else if(z.gt.3500.d0) then
	else if(z.gt.5650.d0) then
491	$y(3) = Tnow * (1.0d0 + z)$
	$y(3) = Tnow * (1.0d0 + z) * 0.62d0$
496	$rhs = dexp(1.5d0 * dLog(CR*Tnow/(1.0d0+z)))$
	$rhs = dexp(1.5d0 * dLog(CR*Tnow*0.62d0/(1.0d0+z)))$
497	$- CB1_He1 / (Tnow * (1.0d0+z)) / Nnow$
	$- CB1_He1 / (Tnow * 0.62d0 * (1.0d0+z)) / Nnow$
505	$y(3) = Tnow * (1.0d0 + z)$
	$y(3) = Tnow * (1.0d0 + z) * 0.62d0$
509	$rhs = dexp(1.5d0 * dLog(CR*Tnow/(1.0d0+z)))$
	$rhs = dexp(1.5d0 * dLog(CR*Tnow*0.62d0/(1.0d0+z)))$
510	$- CB1 / (Tnow * (1.0d0+z)) / Nnow$
	$- CB1 / (Tnow * 0.62d0 * (1.0d0+z)) / Nnow$
525	$Trad = Tnow * (1.0d0 + zend)$
	$Trad = Tnow * (1.0d0 + zend) * 0.62d0$
560	if(z.gt.8000.d0) then
	if(z.gt.13000.d0) then
566	else if(z.gt.3500.d0) then
	else if(z.gt.5650.d0) then
570	$rhs = dexp(1.5d0 * dLog(CR*Tnow/(1.0d0+z)))$
	$rhs = dexp(1.5d0 * dLog(CR*Tnow*0.62d0/(1.0d0+z)))$
571	$- CB1_He2 / (Tnow * (1.0d0+z)) / Nnow$
	$- CB1_He2 / (Tnow * 0.62d0 * (1.0d0+z)) / Nnow$

Continued on next page

Table 3 – continued from previous page

line	recfast
576	else if(z.gt.2000.d0)then
	else if(z.gt.3200.d0)then
579	rhs = dexp(1.5d0 * dLog(CR*Tnow/(1.d0+z))
	rhs = dexp(1.5d0 * dLog(CR*Tnow*0.62d0/(1.d0+z))
580	- CB1_He1/(Tnow*(1.d0+z))) / Nnow
	- CB1_He1/(Tnow*0.62d0*(1.d0+z))) / Nnow
589	rhs = dexp(1.5d0 * dLog(CR*Tnow/(1.d0+z))
	rhs = dexp(1.5d0 * dLog(CR*Tnow*0.62d0/(1.d0+z))
590	- CB1/(Tnow*(1.d0+z))) / Nnow
	- CB1/(Tnow*0.62d0*(1.d0+z))) / Nnow
660	Trad = Tnow * (1.d0+z)
	Trad = Tnow*0.62d0 * (1.d0+z)
805	f(3) = Tnow
	f(3) = Tnow*0.62

References

- [1] K. Abazajian et al., Astron. J. **126**, 2081 (2003).
- [2] J. K. Adelman-McCarthy et al., Astrophys. J. S **175**, 297 (2008).
- [3] J. C. Mather et al., Astrophys. J. **354**, L37 (1990)
- [4] G. F. Hinshaw et.al., Astrophys. J. **208**, 19H (2013).
- [5] P. A. R. Ade et al., Astron. and Astrophys. **571**, A1 (2014).
- [6] S. Perlmutter et al.. Astrophys. J. **517**, 565 (1998).
- [7] A. Riess et al., Astron. J. **116**, 1009 (1998).
- [8] R. Hofmann, Annalen d. Physik **527**, 254 (2015).
- [9] R. Hofmann, *The Thermodynamics of Quantum Yang-Mills Theory: Theory and Applications*, second edition, World Scientific (2016).
- [10] J. A. Frieman, C. T. Hill, A. Stebbins, and I. Waga, Phys. Rev. Lett. **75**, 2077 (1995).
- [11] F. Giacosa and R. Hofmann, Eur. Phys. J. C **50**, 635 (2007).

- [12] S. L. Adler, Phys. Rev. **177**, 2426 (1969)
 S. L. Adler and W. A. Bardeen, Phys. Rev. **182**, 1517 (1969)
- [13] J. S. Bell and R. Jackiw, Nuovo Cim. A **60**, 47 (1969)
- [14] K. Fujikawa, Phys. Rev. Lett. **42**, 1195 (1979).
 K. Fujikawa, K., Phys. Rev. D **21**, 2848 (1980); Erratum-ibid. Phys. Rev. D, **22**, 1499 (1980).
- [15] R. D. Peccei and H. R. Quinn, Phys. Rev. D **16**, 1791 (1977).
 R. D. Peccei and H. R. Quinn, Phys. Rev. Lett. **38**, 1440 (1977).
- [16] B. J. Harrington and H. K. Shepard, Phys. Rev. D **17**, 2122 (1977).
- [17] W. Nahm in *Trieste Group Theor. Method*, p. 189 (1983).
 W. Nahm, Phys. Lett. B **90**, 413 (1980).
 W. Nahm, CERN preprint TH-3172 (1981).
 W. Nahm, *The Construction of all Self-dual Multimonopoles by the ADHM Method in Monopoles in Quantum Field Theory*, ed. N. Craigie *et al.* (World Scientific, Singapore), p. 87 (1982).
- [18] T. C. Kraan and P. Van Baal, Phys. Lett. B **428**, 268 (1998)
 T. C. Kraan and P. Van Baal, Nucl. Phys. B **533**, 627 (1998).
- [19] K. Lee and C. Lu, Phys. Rev. D **58**, 025011-1 (1998).
- [20] C. Wetterich, Phys. Lett. B **522**, 5 (2001).
- [21] J.-L. Bernal, L. Verde, A. G. Riess, JCAP **10**, 019 (2016) [arXiv:1607.05617]
- [22] P. A. R. Ade *et al.*, Astron. & Astrophys. **594**, A13 (2016). [arXiv:1502.01589]
- [23] A. G. Riess *et al.*, Astrophys. J. **826**, 56 (2016). [arXiv:1604.01424]
- [24] J. Beringer *et al.* (Particle Data Group), Phys. Rev. D **86**, 010001 (2012).
- [25] D. J. Fixsen *et al.*, Astrophys. J. **473**, 576 (1996).
- [26] P. A. R. Ade *et al.*, Astron & Astrophys. **571**, A16 (2014). [arXiv:1303.5076v3]
- [27] V. Mukhanov, *Physical Foundations of Cosmology*, Cambridge University Press (2005).
- [28] S. Seager, D. Sasselov, and D. Scott, Astrophys. J. **523**, L1, (1999),
 S. Seager, D. Sasselov, and D. Scott, Astrophys. J. Supp. **128**, 407 (2000),
 W. Y. Wong, A. Moss, and D. Scott, Mon. Not. Roy. Astron. Soc. **386**, 1023 (2008), [arXiv:0711.1357]
 D. Scott and A. Moss, Mon. Not. Roy. Astron. Soc. **397**, 445 (2009).
 [arXiv:0902.3438]

- [29] W. Hu and N. Sugiyama, *Astrophys. J.* **471**, 542 (1996). [arXiv:astro-ph/9510117]
- [30] R. Hofmann, *Nature Phys.* **9**, 686 (2013).
- [31] <http://www.astro.ubc.ca/people/scott/recfast.html>.